IOP Conf. Series: Materials Science and Engineering **110** (2016) 012027 doi:10.1088/1757-899X/110/1/012027

Combined ion (Ar^+, 20 keV) and light irradiation of the quenched Fe-8.25 at % Mn alloy. Separation between thermal and radiation induced long-range effects

V V Ovchinnikov[1, 2], N V Gushchina[1] and S A Bedin[1]

[1] Institute of Electrophysics, Ural Branch of Russian Academy of Sciences, Amundsena Street 106, Yekaterinburg, 620016, Russia
[2] Ural Federal Technical University named after the First President of Russia B.E. Yeltsin, Mira Street 19, Yekaterinburg, 620002, Russia

e-mail: viae05@rambler.ru

Abstract. Mössbauer and X-ray diffraction investigations of the radiation-induced $\alpha \rightarrow \gamma$ phase transformation and short-range-order formation processes in the quenched Fe-8.25 at % Mn alloy under combined exposure (simultaneous visible light and Ar^+ 20-keV ion beam irradiation) are carried out. Combined exposure made it possible to fix the target stationary temperature, and hence, the intensity of thermally-stimulated processes; an energy and ion current density could independently be varied in a wide range. As a result, an important contribution of a non-thermal constituent of ion beam exposure to the structural state of alloy was proved. Only in the presence of ion beam, an $\alpha \rightarrow \gamma$ (bcc $\rightarrow$ fcc) phase transformation and accelerated intraphase processes preparing this transformation are observed in the deep layers of the target (about 10^3 R_p). With allowance for the relatively low level of thermally and radiation-stimulated processes, radiation-dynamic effects associated with propagation of intense post-cascade solitary waves, which can rearrange metastable matters, are considered as the cause of the observed transformations.

Introduction

In the last decades, increasing attention is paid to research in the field of the impact of charged particle (electrons and ions) beams on the surface of a solid. The results of the research are extensively used for the technological purpose, in particular, for the modification of the properties of engineering materials [1, 2].

Information about the impact of accelerated ion beams with energies from a few tens to several hundreds of keV on materials is mainly limited to that about the change in the composition and structure in a very thin surface layer of the matter, the thickness of which is determined by the projected range of bombarding particles. The projected range of ions with the above energies in solids is only from a few tens to several hundreds of nanometers.

Changes in the chemical composition and structure (in the area of ion penetration and its immediate vicinity) are associated with ion implantation, selective ion sputtering of components from the target, the formation of radiation defects, the static stresses arisen from implanted ions, phase formation and dissolution due to radiation-enhanced diffusion, rapid quenching of the target material in the regions of thermal spikes (resulting from the evolution of cascades of atomic displacements), and others [3].

Content from this work may be used under the terms of the Creative Commons Attribution 3.0 licence. Any further distribution of this work must maintain attribution to the author(s) and the title of the work, journal citation and DOI.
Published under licence by IOP Publishing Ltd

At the same time, a number of unusual effects of the "long-range" nature was revealed (at depth up to several hundreds micrometers and more) under ion irradiation [4-9, 11], which has not yet received a full explanation. Effects increasing the impact depth from a few tens projected ranges (R_p) to huge quantities of the order of 10^3-10^5 R_p can be divided into the following groups:

(1) effects related to the peculiarities of motion equations of accelerated ions in crystals (such as channeling and focused substitution), which provide an insignificant increase in the impact depth for heavy ions with low and medium energies to ~5-10 R_p [10, 11];

(2) effects caused by radiation or both radiation and thermally stimulated processes (radiation-enhanced diffusion and tribodiffusion) at a depth to several tens R_p [10, 11];

(3) effects in static stress fields from implanted impurities under *high-dose* irradiation: martensitic transformations at a depth of several R_p [12], generation and movement of dislocations deep into material by several tens of micrometers [4, 5];

(4) radiation-dynamic (RD) effects, which are related with the fact that the cascades of atomic displacements are nanoregions of explosive energy release, the temperature in which can achieve 5000-6000 K and above for 10^{-12} s the rapid expansion of these “thermal spikes” [13] results in the emission of post-cascade shock waves, which initiate the rearrangement of metastable media [7-9, 11, 14] at *lower fluences* (beginning from 10^{14} cm^{-2}) and at the depth of up to 10^3-10^5 R_p.

To understand the nature and to construct the reliable theory for describing RD-processes, they should be thoroughly experimentally investigated. In this case it is necessary to separate thermal from radiation induced long-range effects.

Based on the above, we investigated the regulations of the combined influence of Ar^+ *ion (E=20 keV)* and *light* beams on the *metastable* (quenched from 900°C) Fe-8.25 at % Mn alloy. In the course of the experiment, the *heating rate* and the *steady-state* temperature of the target were fixed at a given level due to the replacement of the ion beam power density P_S (W/cm^2) from 0 to 100% by the light irradiation. As a result, the temperature and the rate of thermal processes was managed to fix on the preassigned level; the energy (E), ion current density (j), and fluence (F) of argon ions could independently be varied in a wide range. Note that according to the equilibrium phase diagram, the Fe-8.25 at % Mn quenched alloy is supersaturated solid solution of manganese in iron, which is metastable.

Experimental

The Fe-8.25 at % Mn alloy under study according to chemical analysis had the following content of impurities: 0.008 C, 0.003 N, 0.007 S, and 0.010 P wt %. The alloy was melted in an induction furnace in the argon atmosphere. The ingots were forged to obtain rods 6×12 mm in cross section and rolled at 1000°C to obtain sheets 0.5 mm thick. Pretreatment consisted of normalizing (900°C), annealing (600°C), and quenching from 850°C (from γ region) in a 15% solution of NaCl. After quenching the alloy has a martensitic structure (100% bcc α'- martensite). Thin foils for Mössbauer studies in transmission geometry were mechanically and electrolytically polished in electrolyte (12 g Cr_2O_3 and 100 mL H_3PO_4). The thickness of the samples was 25 μm.

The samples were irradiated in a continuous mode in the ion implanter equipped with a PEP-18 ion source based on a low-pressure glow discharge with a hollow cold cathode [15]. The power density of the Ar^+ ion beam was 1-2 W/cm^2 at its energy in the range 10-20 keV and current densities from 15 to 75 $\mu A/cm^2$.

We used a visible light source with a comparable power (in the range 0-3 W/cm^2) in the form of an incandescent electric lamp with a reflector forming a parallel beam of light.

The sample temperature was controlled with the help of thin chromel-alumel thermocouples connected with an Advantech Adam 4000 automated system for digital signal registration.

The Mössbauer study was performed using an SM-2201 Mössbauer spectrometer in the constant acceleration mode. Isotope ^{57}Co in Pd was served as the source of γ-quanta. X-ray structural analysis was carried out using a DRON-4M diffractometer. All measurements were done at the room temperature.

Details of exposure, measurements and results

The quenched alloy samples in the form of foils 25 μm thick were irradiated with combined Ar^+ ion and light beams in different modes (Table 1). They were hanged in an implanter's vacuum chamber (P~$5\cdot10^{-5}$ mm Hg) on thin threads with a low heat conductivity so that heat sink (removal) from the samples was carried out almost by the heat radiation only.

In this case, the kinetic curve of the target heated by energy currents has two asymptotes [16] corresponding to the energy conservation principle at $t=0$ (linear growth of temperature T in the absence of thermal radiation) and Stefan-Boltzmann law at $t\to\infty$ in a stationary mode, when $T=const$.

The study of the regularities of initiating and proceeding of RD processes is complicated by the fact that the change in energy E and ion current density j inevitably leads to a change in the target temperature. For example, a change in the ion current density from 15 to 40 μA/cm^2 at the ion energy E = 20 keV leads to a change in the stationary temperature of the foils from about 250 to 380°C[1]. It is very difficult to separate the contribution of RD effects to j and E from the accompanying thermal effects.

In this regard using an additional source of energy, namely, the light beam, the power density introduced into the sample was fixed:

$$P_S = P_S^i + P_S^l = \frac{1}{e} jE + P_S^l ,$$

at the level P_S = 1.5 W/cm^2; where indices i and l mean the ion beam and the light beam, respectively; e is the singly-charged ion charge (e = 1,6·10^{-19} C).

Table 1. Modes of sample processing (T = const = 480°C)

No.	Type of exposure	Parameters of irradiation		
		j, μA/cm^2	E, keV	Fluence F, cm^{-2}
1	Ar^+ ion irradiation	75	20	10^{16}
2	Ar^+ ion irradiation	75	20	$3\cdot10^{17}$
3	Light irradiation	-	-	–
4	Combined irradiation	40	20	10^{16}
5	Combined irradiation	15	20	10^{16}
6	Combined irradiation	75	15	10^{16}
7	Combined irradiation	75	10	10^{16}

The table shows that, every time, any of the parameters j, E, or fluence (F) took two different values when two other parameters were constant. When varying j and E (from maximum to lower values), the respective part of the power that was caught by the target was compensated by a visible light beam.

XRD data suggest that α (bcc) $\rightarrow$ γ (fcc) phase transformation takes place (at a projected range of penetrating ions of only two-three tens no more nanometers) only at ion current density j = 75 μA/cm^2, E = 20 keV in the entire volume of the Fe-8.25%Mn alloy specimens for 20 s and 10 min. In this case, there was no a compensating light beam.

XRD patterns taken from the irradiated and unirradiated sides of the foils include additional weak lines typical of a fcc phase in addition to the lines corresponding to bcc lattice. The most intense of which is the line (220). This shows the long-range nature of the ion bombardment effects on the structure of the Fe-8.25 at % Mn alloy, which initiates the accelerated (already within 20 s of

[1] Stationary temperatures for various metals are different from each other only due to different emissivity α of the metals (in our case $\alpha \approx$ 0.40-0.42).

exposure) γ-phase formation. An increase in the exposure time to 10 min has almost no influence on the diffraction patterns.

It was established that no α (bcc) $\rightarrow$ γ (fcc) phase transition occurred at all lower ion current densities in the presence of the compensating power introduced into the sample by the light beam.

XRD patterns of the samples subjected to the combined exposure are the same that those of the initial sample. They only exhibit the lines of the α (bcc) solid solution. However, this does not exclude the possible intraphase processes of atom redistribution preceding the γ (fcc) phase appearance.

Since the atomic (electron) scattering amplitudes of manganese and iron are very close, the efficiency of XRD methods for the analysis of short-range atomic order in the present case is extremely low. In this regard, the Mössbauer effect was used to investigate the possible redistribution of Mn and Fe atoms in the solid solution and to confirm the fact of the $\alpha \rightarrow \gamma$ structural phase transition at a maximum current density.

Figure 1 demonstrates the Mössbauer spectra of the Fe-8.25 at % Mn alloy (a) in the initial state, after exposure to (b) a light beam (in the absence of ion irradiation), and (c) ion beam irradiation.

The presence of intense paramagnetic line in the central part of the spectra of the samples irradiated with Ar^+ ions (j = 75 μA/cm^2, E = 20 keV) at 480°C for 20 s (Figure 1c) and 10 min confirms the $\alpha \rightarrow \gamma$ (bcc $\rightarrow$ fcc) phase transformation in them with the formation of approximately the same amount of the γ-phase under irradiation in both cases.

Assuming the small difference in the probabilities of the Mössbauer effect for α and γ phases, the areas of respective subspectra were used to find the amount of the precipitated γ phase ~ 8% (in both cases: t = 20 s and 10 min).

Both Mössbauer study and XRD analysis indicate that the samples *heated with a light beam* and held at a temperature of 480°C (in the absence of ion irradiation, Figure 1b) for 10 min and those *subjected to combined exposure* at the same temperature do not exhibit the $\alpha \rightarrow \gamma$ phase transition (they contain only traces of a γ-phase, i.e., retained austenite).

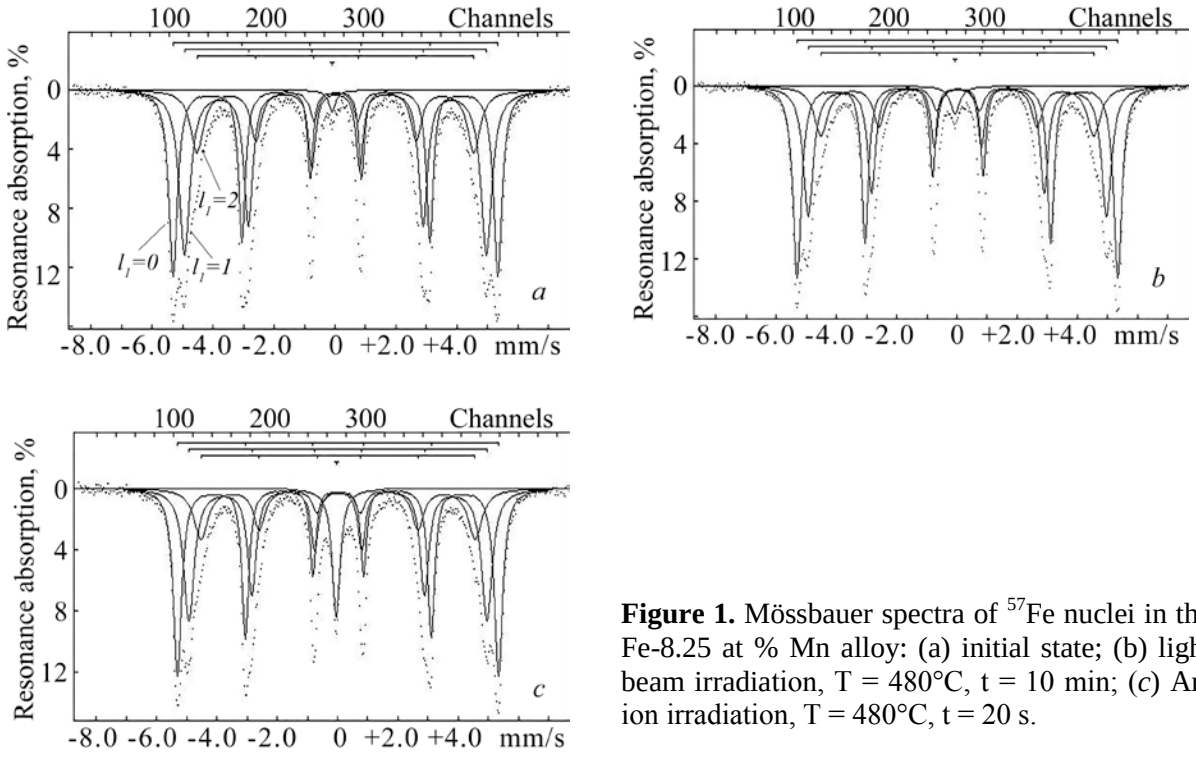

Figure 1. Mössbauer spectra of ^{57}Fe nuclei in the Fe-8.25 at % Mn alloy: (a) initial state; (b) light beam irradiation, T = 480°C, t = 10 min; (*c*) Ar^+ ion irradiation, T = 480°C, t = 20 s.

Although the intensity of the paramagnetic line does not increase after light heating of the samples (in the absence of an ion beam) as well as after different modes of the combined exposure (Table 1), nevertheless, Mössbauer subspectra intensities significantly change. Lines of the subspectra corresponding to $-1/2 \rightarrow -3/2$ nuclear transitions, as components of the outer peak of the experimental spectrum of initial sample are shown in Figure 1a.

The relative intensity of the subspectra corresponding to the Fe atoms, in the first coordination sphere of which there is no Mn atoms (i.e., the number of manganese atoms in the first coordination sphere of iron $l_1 = 0$), increases, as compared with that for the quenched state (Figures 1b, 1c).

The intensities of the components which correspond to the presence of one or two manganese atoms ($l_1 = 1, 2$) near a Fe atom, on the contrary, decrease. The observed changes in the intensities of the subspectra, which are proportional to the respective probabilities $P(l_1)$ showing the presence of l_1 Mn atoms near the Fe atom, indicate the solid solution short-range separation into regions enriched and depleted in manganese under combined irradiation (for 20 s and 10 min) and under sufficiently long (10 min), purely electromagnetic radiation.

As a result of fitting of the Mössbauer spectra with the superposition of Zeeman sextets of lines (corresponding to $l_1 = 0$, 1 and 3), we obtained an average effective magnetic field $\langle H \rangle$ at ^{57}Fe nuclei for various modes of the combined irradiation. Considering the linear relation between $\langle H \rangle$ and Cowley' short-range order parameters on the nearest coordination spheres α_i [17], and taking into account that the influence of the second, third, and more remote spheres for the considered Mn concentration is insignificant [18], short-range atomic order parameters α_1 on the first coordination sphere were calculated.

Parameter α_1 is zero for the initial state and the state after a brief (20 s) light exposure. The value of α_1 becomes positive (short-range decomposition) after ion irradiation, all modes of combined irradiation, and also after prolonged (5 and 10 min) light irradiation (α_1= 0.05 and 0.16). The maximum value of α_1 for all kinds of radiation used is + 0.16 –+0.17 with an error ± 0.02. To achieve this degree of short-order separation, 20 s is enough upon argon ion irradiation and all modes of combined exposure (a further exposure up to 10 min change nothing). Upon light irradiation, in the absence of ion bombardment, this requires at least 10 min. The latter indicates that the combined irradiation (when there is a certain fraction of the power of the ion beam) leads to a substantial increase in the rate of short range order formation in the sample volume.

Note that the Mössbauer effect in transmission geometry gives information about the whole volume of the sample (foil 25 μm thick in our case), since a fraction of resonant nuclei, which are located in the area of ion path (no more than 20-30 nm) is less than 0.1% and does not provide a significant contribution to the spectrum.

Conclusions

It was established that under thermal exposure modes being the same, $\alpha \rightarrow \gamma$ (bcc→fcc) phase transformation took place over the entire depth of 25-μm-thick target of the Fe-8.25 at %Mn alloy *only at maximum* ion energy E = 20 keV and ion current density j = 75 μA/cm^2 under irradiation for 20 s and 10 min. This means that only those parameters of the Ar^+ ion beams exceed a certain threshold values (E^* and j^*).

This result is principally important. The fact that this is the *only single set* of parameters at which the transformation takes place is accidental to a certain extent, since the range of variation and the specific values E, j and F have been chosen arbitrarily. In addition, it was found that the exposure to argon ion beam repeatedly (in dozens of times) accelerates the process of short-order separation of the alloy. It can be argued based on these results that the lower threshold of the ion current density, which provides the multiple acceleration of intraphase separation j^{**}, does not exceed 15 μA/cm^2 and the lower energy threshold E^{**} does not exceed 10 keV.

According to the obtained data, the fluence threshold causing phase and intraphase processes does not exceed 10^{16} cm^{-2}. In general, the question about threshold values of the considered parameters (including their interdependence) is difficult enough and a further research is needed to clarify it.

Under the same heating modes for all samples, the obtained data are unambiguous evidence of the existence of a nonthermal component in the ion beam effect, which initiates the $\alpha \rightarrow \gamma$ phase transformation over the entire depth of the target (about 10^3 R_p) and accelerates the intraphase processes foregoing to them.

With allowance for the fact that: (1) all radiation defects form under ion bombardment in the ion path zone (i.e. in the layer with a thickness below than 0.03 μm); (2) the concentration of interstitial atoms and vacancies survived in atomic displacement cascades does not exceed 0.01 % of the total number of atoms in the target; (3) diffusion length of vacancies does not exceed 1 μm for 20 s; (4) there are a large number of traps and sinks for point defects in the initial quenched alloy; it allows us to draw the conclusion that the steep increase in the rate of structural-phase transformations under ion beam exposure can hardly be explained by only radiation-enhanced diffusion mechanism. Is excluded also the role of thermally-activated process, because the temperature was the same for the combined beams and a light beam.

With that said, the observed transformations can be considered as the additional evidence in favor of the radiation-dynamic mechanism [7-9, 11, 14, 19] of accelerated ions effects on the substances.

Acknowledgments
This work was supported by the Russian Scientific Foundation, project no. 15-19-10054.

References

[1] Proceedings of 12th International Conference on Modification of Materials with Particle Beams and Plasma Flows. 2014 (Tomsk. September 21-26)
[2] Nastasi M and Mayer J W 2006 *Ion Implantation and Synthesis of Materials* (Springer Series in Materials Science)
[3] Ovchinnikov V V 1996 *Izvestiya RAN, Metally* **6** 104
[4] Didenko A N, Kozlov E V, Sharkeev Yu N, Tailashev A S, Rajabchikov A I, Pranjavichus L and Augulis L 1993 *Surface and Coatings Technology* **56** 97
[5] Sharkeev Yu P and Kozlov E V 2002 *Surface and Coatings Technology* **158-159** 219
[6] Tetelbaum D I, Azov A Yu, Kurilchik E V et al 2003 *Vacuum* **70** 169
[7] Borodin S N, Kreindel Yu E, Mesyats G A and Ovchinnikov V V 1989 *Technical Physics Letters* **15** 13 87
[8] Kreindel Yu E and Ovchinnikov V V 1990 *Vacuum* **42** 81
[9] Ovchinnikov V V, Chernoborodov V I and Ignatenko Yu G 1995 *Nucl.Instrum. and Meth. in Phys.Res. B* **103** 313
[10] Ryssel H and Ruge I *Ionenimplantation* ((Chichester: Wiley, 1986)
[11] Goloborodsky B Yu, Ovchinnikov V V and Semenkin V A 2001 *Fusion Technology* **39** 1217
[12] Johnson E, Johansen A, Sharlot-Kristesen L. et. al. 1967 *Nucl. Instr. and Meth. in Phys. Res. B* **19-20** 171
[13] Ovchinnikov V V, Makhin'ko F F, Solomonov V I, Gushchina N V and Kaigorodova O A 2012 *Technical Physics Letters* **38** 86
[14] Ovchinnikov V V 2008 *Physics-Uspekhi* **51** 955
[15] Gavrilov N V, Mesyats G A, Nikulin S P, Radkovskii G V, Eklind A and Perry A J 1996 *J. Vac. Sci. Technol. A* **14** 1050
[16] Ovchinnikov V V, Ovchinnikov S V, Makhin'ko F F and Povzner A A 2011 *Izv. Vyssh. Uchebn. Zaved. Fiz.* **54** 1/3 101
[17] Ovchinnikov V V 2006 *Mossbauer Analysis of the Atomic and Magnetic Structure of Alloys* (Cambridge Int. Sci. Publ. Cambridge. UK)
[18] Litvinov V S, Ovchinnikov V V, Dovgopol S P and Karakishev S D 1979 *Fiz. Met. Metalloved.* **47** 1 96
[19] Ovchinnikov V V 1994 in: Proc. XVI International Symposium on Discharges and Electrical Insulation in Vacuum **2259** ed. Mesyats G A (Moscow-St. Petersburg. SPIE) pp. 605-608